NEURORADIOLOGY
Iran J Radiol. 2022 October; 19(4):e118135. https://doi.org/10.5812/iranjradiol-118135.
Published online 2022 December 25. **Research Article**

Correlation of Diffusion Tensor Imaging Parameters with the Pathological Grade of Brain Glioma and Expression of Vascular Endothelial Growth Factor and Ki-67

Jing Wu [1,*], Wanshu Peng [2], Taisong Peng [3], Zhigao Xu [3] and Ziqing Ye [1]

[1] Beijing Huairou Hospital, Beijing, China
[2] The First Affiliated Hospital of Dalian Medical University, Dalian, China
[3] Datong Third People's Hospital, Datong, China

[*] *Corresponding author*: Beijing Huairou Hospital, Beijing, China. Email: kurtwatkinsltw@yahoo.com

Received 2021 August 13; **Revised** 2022 September 07; **Accepted** 2022 September 12.

Abstract

Background: Most brain gliomas are high-grade and likely to spread locally. Consequently, these patients commonly have a poor prognosis. Accurate identification of the malignancy grade of brain glioma before treatment is of great clinical significance.
Objectives: This study aimed to explore the correlation of diffusion tensor imaging (DTI) parameters, fractional anisotropy (FA), and apparent diffusion coefficient (ADC) with the pathological grade of brain glioma and expression of vascular endothelial growth factor (VEGF) and Ki-67.
Patients and Methods: A total of 116 patients were selected for this study from January 2018 to December 2019. All the participants underwent magnetic resonance imaging (MRI) and DTI before surgery, and the FA and ADC values were measured for the regions of interest. Surgically resected tumor specimens were collected for immunohistochemical assay. Finally, the FA and ADC values and positive expression rates of VEGF and Ki-67 were compared.
Results: A significantly higher FA, besides the positive expression of VEGF and Ki-67, was reported in the high-grade group, whereas a lower ADC was found in this group compared to the low-grade group ($P < 0.05$). Areas of normal white matter and peritumoral edema had higher FA values, whereas lower ADCs were measured in these areas compared to the cerebrospinal fluid ($P < 0.05$). The FA of tumor parenchymal area was positively correlated with the World Health Organization (WHO) class of tumors ($r = 0.588$, $P = 0.028$), and the expression of VEGF and Ki-67 was positively correlated with the WHO grade ($r = 0.843$, $P = 0.002$ and $r = 0.743$, $P = 0.006$, respectively). The FA of tumor parenchymal area was positively correlated with the expression of VEGF and Ki-67 ($r = 0.654$, $P = 0.008$ and $r = 0.567$, $P = 0.012$, respectively). However, the ADC of tumor parenchymal area was not significantly correlated with the WHO grade, VEGF expression, or Ki-67 expression ($r = 0.143$, $P = 0.156$, $r = 0.232$, $P = 0.116$, and $r = 0.054$, $P = 0.179$, respectively).
Conclusion: The FA value, as a DTI parameter, is valuable for assessing the malignancy grade of tumor cells and can provide a proper reference for formulating treatment regimens for brain gliomas.

Keywords: Brain Glioma, Diffusion Tensor Imaging, Vascular Endothelial Growth Factor, Ki-67

1. Background

Brain glioma is the most common primary craniocerebral tumor, caused by the progression of cancer in glial cells in the spinal cord. Patients mainly experience headache, seizures, nausea, vomiting, hemidysesthesia, and blurred vision. Besides, this type of tumor seriously affects the function of local brain tissues (1, 2). Most brain gliomas are high-grade and likely to spread locally; consequently, patients commonly have a poor prognosis. Since different grades of brain gliomas have different treatment options, accurate identification of the malignancy grade before treatment is of great clinical significance (3-5).

Magnetic resonance imaging (MRI) can be used to determine the location of brain tumors, invasiveness of tumors into the surrounding normal brain tissues, and source and type of tumor tissue (6). However, it cannot accurately represent the pathological grade or microscopic histological characteristics of tumors, which in turn increases the difficulty of formulating a suitable treatment regimen and directly affects the patient prognosis (7). Therefore, it is necessary to find an approach that can accurately reflect the pathological features of tumors.

Diffusion tensor imaging (DTI) is derived from diffusion-weighted imaging (DWI). The DTI parame-

ters can be used to reflect the diffusion of water molecules in brain tissues, which is valuable for assessing the grade of brain glioma, integrity of nerve fiber bundles, and peritumoral edema (8). As vascular endothelial growth factor (VEGF) can promote neovascularization, it plays a pivotal role in the progression of multiple malignancies (9, 10). Additionally, Ki-67 is a nuclear proliferation-related antigen, the expression of which is closely associated with the proliferation of tumor cells (11).

2. Objectives

This study aimed to investigate the correlation of DTI parameters with the pathological parameters of brain glioma and VEGF and Ki-67 expression to provide a reference for formulating early diagnosis and treatment plans for brain glioma.

3. Patients and Methods

3.1. Baseline Clinical Data

A total of 116 patients with brain glioma, confirmed by a pathological examination in Beijing Huairou Hospital (Beijing, China) from January 2018 to December 2019, were enrolled in this study. The inclusion criteria were as follows: undergoing DTI; images of ideal quality; and brain glioma confirmed by a pathological examination. On the other hand, patients with other craniocerebral tumors were excluded. This study was approved by the hospital ethics committee [approval No.: Beijing (Huairou)-2019-006-01]. The ethical approval file was not available online at the time of approval (in 2018), and it is not linked to a webpage. Written informed consent was obtained from all the participants in this study.

3.2. Imaging Examination

All the participants were examined using a MAGNETOM Verio 3.0T MRI system (Siemens, Germany). First, conventional MRI was performed, and all patients underwent conventional plain and contrast-enhanced T1-weighted imaging (T1WI) and T2WI scanning. The conventional MRI scanning parameters were as follows: slice thickness, 5.0 mm; interslice gap, 1.5 mm; and matrix size, 256 × 256. Also, the T1WI parameters were as follows: field of view (FOV), 175 × 220 mm; repetition time/echo time (TR/TE), 225/2.5 ms; flip angle, 150°; and bandwidth, 184. Besides, the turbo spin echo T2WI parameters were as follows: FOV, 240 × 240 mm; TR/TE, 5,000/102 ms; flap angle, 179°; and bandwidth, 210. Whole-brain coverage was acquired with 40 slices on T1WI and with 80 slices on T2WI.

All the patients received a contrast agent injection at 0.1 mmol/kg (gadodiamide, GE Healthcare, USA) through the anterior elbow vein and underwent FLASH contrast-enhanced scanning with the following parameters: TR, 1,660 ms; TE, 2.95 ms; inversion time (TI), 900 ms; slice thickness, 1 mm; and interslice gap, 0 mm. Whole-brain coverage was acquired with 144 slices. Additionally, for DTI scanning, echo-planar imaging (EPI) cross-sectional scanning was conducted under the following parameters: TR, 7,400 ms; TE, 87 ms; slice thickness, 3 mm; interslice gap, 0 mm; FOV, 230 × 230 mm; and matrix size, 128 × 128. For whole-brain coverage, 40 slices were used, with b values of 0 s/mm^2 and 1,000 s/mm^2. Besides, diffusion-sensitizing gradients were applied in 20 directions to collect signals four times for 332 seconds, and the results were averaged (12, 13).

3.3. Processing of Imaging Data

The scanning data were transmitted to a workstation (Siemens, Germany), and fractional anisotropy (FA) and apparent diffusion coefficient (ADC) maps were automatically generated through smoothing and interpolation using a supporting software package (Syngo MRB17). According to contrast-enhanced T2WI or T1WI findings, the largest representative tumor slice was selected for each patient, and peritumoral edema, tumor parenchymal, cerebrospinal fluid, and white matter areas on the opposite side of the same anatomical site (normal brain) were considered as the regions of interest (ROIs), which were 20 - 40 pixels in size. They were measured three times based on experience, and the average values were calculated. Finally, the FA and ADC values of each ROI were calculated. The procedures were conducted by the same radiologist with 10 years of experience in analyzing images.

3.4. Detection of VEGF and Ki-67 Expression in Pathological Tissues

Pathological tissues were surgically resected from all the patients, routinely fixed, and embedded in paraffin. The produced sections were deparaffinized using xylene solution, hydrated in gradient concentrations of ethanol solution, and added dropwise added 3% hydrogen peroxide to reduce the activity of endogenous peroxidase, followed by Heat-induced using ethylenediaminetetraacetic acid. Next, mouse anti-human VEGF antibody and Ki-67 antibody (Beijing Zhongshan Golden Bridge Biotechnology Co., Ltd., China) were added dropwise and incubated overnight at 4°C. After color was developed using 3,3-diaminobenzidine (DAB), the sections were counterstained with hematoxylin, dehydrated in gradient concentrations of ethanol solutions, transparentized with xylene solution, and mounted with neutral resin.

Five FOVs were randomly selected under a high-power microscope (400X magnification). The brownish yellow color in the cytoplasm and nucleus suggested VEGF- and Ki-67-positive staining, respectively. The VEGF expression was assessed using a semi-quantitative scoring method. First, a score was assigned based on the percentage of positive cells: 0, 0 - 10%; 1, 11 - 25%; 2, 26 - 50%; 3, 51 - 75%; and 4, 76 - 100%. Next, the staining intensity was rated as follows: 0, no positive staining; 1, pale yellow staining; 2, yellow staining; and 3, brownish yellow staining. The final score was obtained on the basis of percentage of positive cells and staining intensity; final scores of $\geq$ 4 and < 4 were considered as positive and negative results, respectively. The positive expression of Ki-67 was directly determined by the percentage of positive cells; the percentage of positive cells $\geq$ 10% indicated positive expression, while < 10% suggested negative expression.

3.5. Observation Indices

The signals in the FA and ADC maps of each ROI were first observed for patients with different pathological grades. Next, the FA and ADC values and the positive expression rates of VEGF and Ki-67 in the tumor parenchymal area were compared. Finally, differences in the FA and ADC values among different ROIs in the same patient were analyzed.

3.6. Statistical Analysis

All data were statistically analyzed in SPSS version 23.0 (released in 2015, IBM SPSS Statistics for Windows, IBM Corp., Armonk, NY, USA). Numerical data, including the positive expression rates of VEGF and Ki-67 and sex ratio, were expressed as rate (%) and compared using χ^2 test. The normal distribution of the collected data was assessed using Kolmogorov-Smirnov test, and all data were found to be normally distributed. The ADC value, FA value, and other quantitative data are presented as mean ± standard deviation (SD). Comparison of FA and ADC values between different ROIs was performed using analysis of variance (ANOVA), and pairwise comparisons between groups were performed by post hoc test. Moreover, Spearman's test was conducted to explore the correlation between the ADC and FA values and expression rates of VEGF and Ki-67. A P-value less than 0.05 was considered statistically significant.

4. Results

4.1. General Clinical Data

This study was performed on 116 patients, including 62 males and 54 females, with a mean age of 42.34 ± 8.87 years (age range, 18 - 76 years). According to the 2016 World Health Organization (WHO) Classification of Tumors of the Central Nervous System (14), there were 10 cases of grade 1 tumor, 32 cases of grade 2 tumor, 26 cases of grade 3 tumor, and 48 cases of grade 4 tumor. Grade 1 and 2 tumors were classified into the low-grade group (n = 42), which consisted of 24 males and 18 females, with a mean age of 42.07 ± 8.13 years (age range, 18-76 years). Grade 3 and 4 tumors were classified into the high-grade group (n = 74), including 38 males and 36 females, with a mean age of 42.53 ± 8.98 years (age range, 18 - 76 years). The sex ratio, age, and other general characteristics of the patients were not significantly different between the high- and low-grade groups (P > 0.05) (Table 1). The typical images of the patients are presented in Figure 1.

4.2. FA and ADC Map Signals

In the FA map of all patients, the tumor parenchymal area, peritumoral edema area, and normal white matter area showed uneven low-intensity signal, uneven high-intensity signal, and uniform high-intensity signal patterns, respectively. In the ADC map, high-intensity signals were observed in the tumor parenchymal, peritumoral edema, and cerebrospinal fluid areas in the low-grade group, whereas the high-grade group showed uneven low-intensity signals in the tumor parenchymal area, high-intensity signals in the peritumoral edema area and cerebrospinal fluid area, and isointense signals in the normal white matter area.

4.3. Relationship of Pathological Grade with FA and ADC Values of Tumor Parenchymal Area

The high-grade group showed a significantly higher FA value and a lower ADC compared to the low-grade group (P < 0.001) (Table 2).

4.4. Correlation of Pathological Grade with VEGF and Ki-67 Expression

The positive expression rates of VEGF and Ki-67 were significantly higher in the high-grade group compared to the low-grade group (P < 0.05) (Table 3).

4.5. FA and ADC Values of Different ROIs

The ADCs were significantly different between various ROIs (P < 0.05). The normal white matter and peritumoral edema areas showed higher FA values, but lower ADCs compared to the cerebrospinal fluid area (P < 0.05). Significant differences were found based on pairwise comparisons between the normal white matter, peritumoral edema, and tumor parenchymal areas (P < 0.05) (Table 4).

Table 1. General Clinical Findings of the Patients

Groups	High-grade (n = 74)	Low-grade (n = 42)	Statistical significance level	P-value
Sex			$\chi^2 = 0.361$	0.548
Male	38	24		
Female	36	18		
Mean age (y)	42.53 ± 8.98	42.07 ± 8.13	$t = 0.274$	0.784

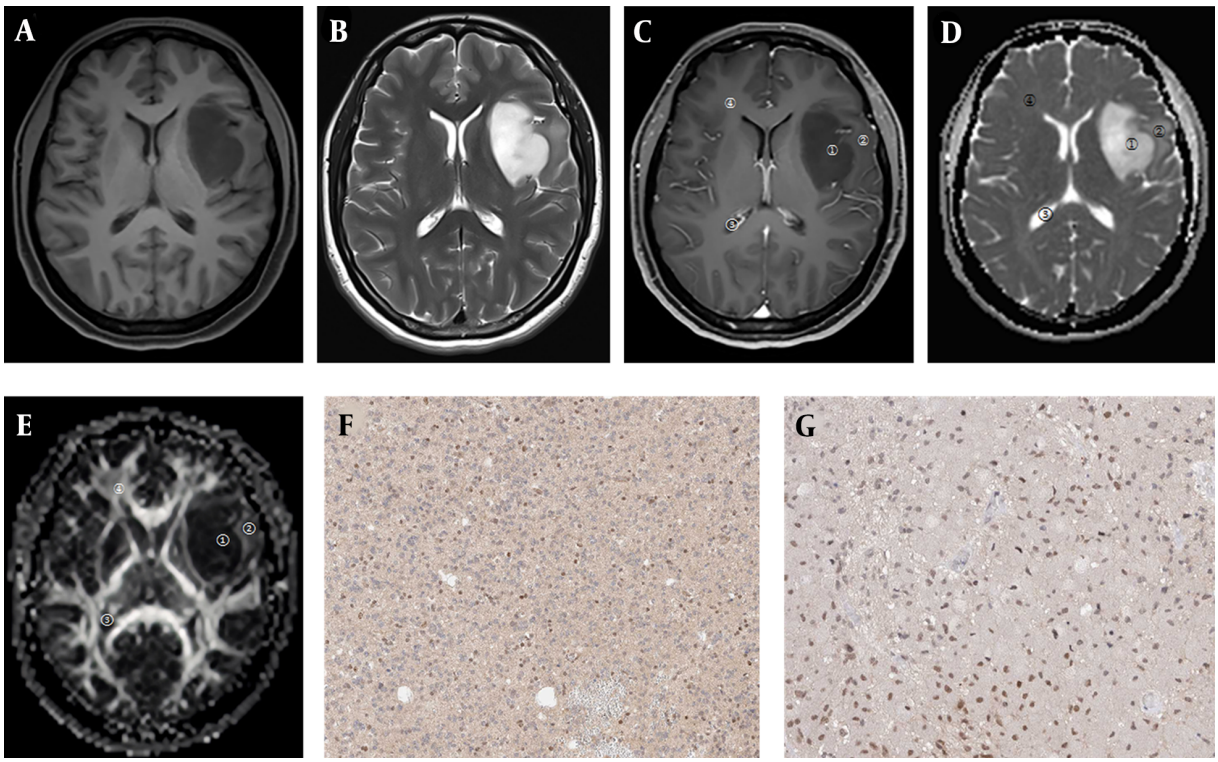

Figure 1. Images of a 40-year-old female patient with the WHO grade II left temporal lobe astrocytoma. A, T1WI tumor lesion area shows low signal intensity; B, T2WI tumor lesion area shows high signal intensity; C, Contrast-enhanced image shows no obvious enhancement; D, In the apparent diffusion coefficient (ADC) map, both tumor parenchymal area and peritumoral edema area show high signal intensities; E, In the fractional anisotropy (FA) map, the tumor parenchymal area shows an uneven low signal intensity pattern, and the peritumoral edema area shows an uneven and slightly high signal intensity pattern (ROI 1, tumor parenchymal area; ROI 2, peritumoral edema area; ROI 3, cerebrospinal fluid area; ROI 4, contralateral normal white matter area); F, Positive vascular endothelial growth factor (VEGF) expression; G, Positive Ki-67 expression.

Table 2. Comparison of FA and ADC Values Between High- and Low-Grade Gliomas in the Tumor Parenchymal Area

Group	FA value	ADC ($\times 10^{-6}$ mm^2/s)
High-grade (n = 74)	0.197 ± 0.032	1014.18 ± 89.29
Low-grade (n = 42)	0.141 ± 0.028	1445.28 ± 91.27
T	9.466	24.792
P	< 0.001	< 0.001

Abbreviations: ADC, apparent diffusion coefficient; FA, fractional anisotropy.

4.6. Correlations of DTI and Pathological Parameters

The FA value of the tumor parenchymal area had a significant positive correlation with the WHO grade of tumors (r = 0.588, P = 0.028). Also, the expression of VEGF and Ki-67 had a significant positive correlation with the WHO grade of tumors (r = 0.843, P = 0.002 and r = 0.743, P = 0.006, respectively). Moreover, the FA value of the tumor parenchymal area had a significant positive correlation with the expression of both VEGF and Ki-67 (r = 0.654, P = 0.008 and r = 0.567, P = 0.012, respectively). The ADC value of the tumor parenchymal area was not significantly correlated with the WHO grade of tumors, VEGF expression, or Ki-67 expression (r = 0.143, P = 0.156, r = 0.232, P = 0.116, and r = 0.054, P = 0.179, respectively) (Table 5).

Table 3. Comparison of VEGF and Ki-67 Expression Between High- and Low-Grade Gliomas

Groups	VEGF		Ki-67	
	Negative	Positive	Negative	Positive
High-grade (n = 74)	5 (6.76)	69 (93.24)	24 (32.43)	50 (67.57)
Low-grade (n = 42)	25 (59.52)	17 (40.48)	26 (61.90)	16 (38.10)
$\chi 2$	38.909		9.490	
P	< 0.001		0.002	

Abbreviation: VEGF, vascular endothelial growth factor.

Table 4. The FA and ADC Values of Different ROIs

ROI	FA value	ADC ($\times 10^{-6}$ mm^2/s)
Normal white matter	0.404 ± 0.011 [a, b]	655.41 ± 54.29 [a, b]
Peritumoral edema area	0.224 ± 0.019 [a]	873.23 ± 92.18 [a]
Tumor parenchymal area	0.129 ± 0.014 [a, b]	1578.42 ± 90.26 [a, b]
Cerebrospinal fluid area	0.116 ± 0.013	1502.91 ± 90.22
F	8.298	14.398
P	< 0.001	< 0.001

Abbreviations: ADC, apparent diffusion coefficient; FA, fractional anisotropy; ROI, region of interest.
[a] P < 0.05, compared to the cerebrospinal fluid area.
[b] P < 0.05, compared to the tumor parenchymal area.

5. Discussion

DTI is developed from DWI with directional gradient magnetic fields. The FA and ADC maps are obtained through recombination of DWI images, indicating the diffusion features (15). DTI focuses on the motion anisotropy of water molecules, involving two independent parameters, namely, ADC and FA. The former represents the diffusivity of water molecules, while the latter is used to quantify the anisotropy of water molecules. The FA value is affected by the density of tumor cells, integrity of the white matter fiber myelin sheath, and tumor extracellular matrix (16). The malignancy grade of glioma cells is usually rated based on nuclear atypia, mitosis, and endothelial status (necrosis/viability). Changes in these characteristics influence the FA and ADC values. Therefore, it is highly reliable to determine the malignancy grade of tumor cells by measuring the FA and ADC values (17).

In this study, the FA and ADC values varied among patients with gliomas characterized by different degrees of malignancy, which is consistent with previous research (18). The observed differences may be attributed to differences in the severity of damage to the surrounding tissues by tumors with various grades of malignancy, invasive growth, and edema. Compared to low-grade glioma cells, high-grade glioma cells exhibit more obvious invasive growth and edema and cause more severe damage to the surrounding tissues. Therefore, high-grade gliomas have higher FA values and lower ADCs. These values differ among various ROIs, probably because the structures of cells and tissues are destroyed by tumor cells (19).

VEGF directly contributes to tumor neovascularization as the main route for tumors to receive hydrogen and nutrients, which is also dominant in tumor invasion and metastasis. Consequently, the expression of VEGF is closely associated with the progression of malignant tumors (20-22). Generally, Ki-67 can reflect the proliferation of tumor cells. Its expression can be detected in G1, S, G2, and M phases, while it quickly disappears in the late M phase. Moreover, Ki-67 has a short half-life, and cell proliferation can be determined by measuring its expression level (23). This study revealed that the positive expression rates of VEGF and Ki-67 were significantly higher in the high-grade group compared to the low-grade group (P < 0.05), mainly because high-grade brain gliomas were more susceptible to neovascularization, and tumor cells proliferated more vigorously. However, the correlation between the ADC value and Ki-67 expression remains controversial. In this regard, Martino et al. reported that the ADC value was negatively correlated with Ki-67 expression (24), whereas Engelhorn et al. found no obvious correlation between the ADC and Ki-67 expression (25); the difference observed in the ROI selection may yield different results due to the heterogeneity of tumors.

Based on the findings, the FA value of DTI is of great significance for glioma diagnosis regarding the following aspects. First, the FA value is highly reliable for the evaluation of tumor cell malignancy and aids in the preoperative grading of gliomas and differential diagnosis of low- and high-grade gliomas. Second, the FA value is not only affected by the content of extracellular water molecules, but also related to the destruction and displacement of white matter bundles due to tumor cell invasion. Therefore, the FA value can reflect peritumoral edema to a certain extent and is conducive to determining tumor invasion. Third, the FA value allows for a non-invasive evalu-

Table 5. Correlation Between DTI Parameters and Pathological Parameters

	WHO grade	VEGF	Ki-67
FA value of tumor parenchymal area	r = 0.588, P = 0.028	r = 0.654, P = 0.008	r = 0.567, P = 0.012
VEGF	r = 0.843, P = 0.002	-	-
Ki-67	r = 0.743, P = 0.006	-	-
ADC of tumor parenchymal area	r = 0.143, P = 0.156	r = 0.232, P = 0.116	r = 0.054, P = 0.179

Abbreviations: ADC, apparent diffusion coefficient; FA, fractional anisotropy; VEGF, vascular endothelial growth factor; WHO, World Health Organization.

ation of the pathological characteristics of tumor tissues before operation, thereby providing valuable information for the formulation and implementation of surgical regimens. Fourth, the FA value provides a basis for the selection of target areas and reduces unnecessary damage in radiotherapy. Fifth, DTI is sensitive to changes in the diffusion of water molecules, which plays a crucial role in monitoring the treatment outcomes (26, 27). Therefore, it can be used as a sensitive index for determining recurrence and evaluating prognosis.

In conclusion, the FA value as a DTI parameter is highly valuable for assessing the malignancy grade of tumor cells and is applicable for the clinical diagnosis and treatment of brain glioma.

Acknowledgments

This study was not financially supported.

Footnotes

Authors' Contribution: Study concept and design, Jing Wu and Wanshu Peng; Analysis and interpretation of data, Taisong Peng; Drafting of the manuscript, Zhigao Xu; Critical revision of the manuscript for important intellectual content, Taisong Peng, Zhigao Xu, and Ziqing Ye; and Statistical analysis, Jing Wu.

Conflict of Interests: The authors have no conflicts of interest to declare.

Data Reproducibility: All data are available from the corresponding author upon reasonable request.

Ethical Approval: This study was approved by the ethics committee of the hospital [approval No.: Beijing (Huairou)-2019-006-01, on the left side of the official stamp].

Funding/Support: There was no funding/support for this study.

Informed Consent: Written informed consent was obtained from all the patients.

References

1. Sommer CJ. Ischemic stroke: experimental models and reality. *Acta Neuropathol*. 2017;**133**(2):245–61. [PubMed ID: 28064357]. [PubMed Central ID: PMC5250659]. https://doi.org/10.1007/s00401-017-1667-0.
2. Jue TR, Sena ES, Macleod MR, McDonald KL, Hirst TC. A systematic review and meta-analysis of topoisomerase inhibition in pre-clinical glioma models. *Oncotarget*. 2018;**9**(13):11387–401. [PubMed ID: 29541421]. [PubMed Central ID: PMC5834287]. https://doi.org/10.18632/oncotarget.24334.
3. Tsoli M, Liu J, Franshaw L, Shen H, Cheng C, Jung M, et al. Dual targeting of mitochondrial function and mTOR pathway as a therapeutic strategy for diffuse intrinsic pontine glioma. *Oncotarget*. 2018;**9**(7):7541–56. [PubMed ID: 29484131]. [PubMed Central ID: PMC5800923]. https://doi.org/10.18632/oncotarget.24045.
4. Yan J, Wen J, Wei ZD, Li XS, Li P, Xiao SW. Prognostic and clinicopathological value of melanoma-associated antigen D4 in patients with glioma. *Oncol Lett*. 2018;**15**(4):4151–60. [PubMed ID: 29541180]. [PubMed Central ID: PMC5835852]. https://doi.org/10.3892/ol.2018.7884.
5. Dabrowski MJ, Draminski M, Diamanti K, Stepniak K, Mozolewska MA, Teisseyre P, et al. Unveiling new interdependencies between significant DNA methylation sites, gene expression profiles and glioma patients survival. *Sci Rep*. 2018;**8**(1):4390. [PubMed ID: 29535343]. [PubMed Central ID: PMC5849697]. https://doi.org/10.1038/s41598-018-22829-1.
6. Jalilianhasanpour R, Beheshtian E, Ryan D, Luna LP, Agarwal S, Pillai JJ, et al. Role of Functional Magnetic Resonance Imaging in the Presurgical Mapping of Brain Tumors. *Radiol Clin North Am*. 2021;**59**(3):377–93. [PubMed ID: 33926684]. https://doi.org/10.1016/j.rcl.2021.02.001.
7. Shahzad K, Mati W. Advances in magnetic resonance imaging (MRI). In: Ahmed W, Phoenix DA, Charalambous CP, editors. *Advances in Medical and Surgical Engineering*. Massachusetts, USA: Academic Press; 2020. p. 121–42. https://doi.org/10.1016/b978-0-12-819712-7.00009-7.
8. Engwer C, Knappitsch M, Surulescu C. A multiscale model for glioma spread including cell-tissue interactions and proliferation. *Math Biosci Eng*. 2016;**13**(2):443–60. [PubMed ID: 27105989]. https://doi.org/10.3934/mbe.2015011.
9. Yu X, Wang W. Tumor suppressor microRNA-613 inhibits glioma cell proliferation, invasion and angiogenesis by targeting vascular endothelial growth factor A. *Mol Med Rep*. 2017;**16**(5):6729–35. [PubMed ID: 28901424]. [PubMed Central ID: PMC5865827]. https://doi.org/10.3892/mmr.2017.7422.
10. Yazdani Y, Sharifi Rad MR, Taghipour M, Chenari N, Ghaderi A, Razmkhah M. Genistein Suppression of Matrix Metalloproteinase 2 (MMP-2) and Vascular Endothelial Growth Factor (VEGF) Expression in Mesenchymal Stem Cell Like Cells Isolated from High and Low Grade Gliomas. *Asian Pac J Cancer Prev*. 2016;**17**(12):5303–7. [PubMed ID: 28125877]. [PubMed Central ID: PMC5454674]. https://doi.org/10.22034/apjcp.2016.17.12.5303.

11. Cordier D, Schädelin S, Duffau H. Influence of 1p19q status and Ki67 index to predict extent of resection in WHO grade II gliomas: a virtual patient model. *J Neurooncol*. 2015;**123**(2):317–8. [PubMed ID: 25917059]. https://doi.org/10.1007/s11060-015-1790-5.
12. Han Y, Wang T, Wu P, Zhang H, Chen H, Yang C. Meningiomas: Preoperative predictive histopathological grading based on radiomics of MRI. *Magn Reson Imaging*. 2021;**77**:36–43. [PubMed ID: 33220449]. https://doi.org/10.1016/j.mri.2020.11.009.
13. Maekawa T, Hori M, Murata K, Feiweier T, Kamiya K, Andica C, et al. Differentiation of high-grade and low-grade intra-axial brain tumors by time-dependent diffusion MRI. *Magn Reson Imaging*. 2020;**72**:34–41. [PubMed ID: 32599021]. https://doi.org/10.1016/j.mri.2020.06.018.
14. Louis DN, Perry A, Reifenberger G, von Deimling A, Figarella-Branger D, Cavenee WK, et al. The 2016 World Health Organization Classification of Tumors of the Central Nervous System: a summary. *Acta Neuropathol*. 2016;**131**(6):803–20. [PubMed ID: 27157931]. https://doi.org/10.1007/s00401-016-1545-1.
15. Chianca V, Albano D, Messina C, Cinnante CM, Triulzi FM, Sardanelli F, et al. Diffusion tensor imaging in the musculoskeletal and peripheral nerve systems: from experimental to clinical applications. *Eur Radiol Exp*. 2017;**1**(1):12. [PubMed ID: 29708174]. [PubMed Central ID: PMC5909344]. https://doi.org/10.1186/s41747-017-0018-1.
16. Davanian F, Faeghi F, Shahzadi S, Farshifar Z. Diffusion Tensor Imaging for Glioma Grading: Analysis of Fiber Density Index. *Basic Clin Neurosci*. 2017;**8**(1):13–8. [PubMed ID: 28446945]. [PubMed Central ID: PMC5396168]. https://doi.org/10.15412/j.bcn.03080102.
17. Shan W, Wang XL. Clinical application value of 3.0T MR diffusion tensor imaging in grade diagnosis of gliomas. *Oncol Lett*. 2017;**14**(2):2009–14. [PubMed ID: 28781644]. [PubMed Central ID: PMC5530196]. https://doi.org/10.3892/ol.2017.6378.
18. Piper RJ, Mikhael S, Wardlaw JM, Laidlaw DH, Whittle IR, Bastin ME. Imaging signatures of meningioma and low-grade glioma: a diffusion tensor, magnetization transfer and quantitative longitudinal relaxation time MRI study. *Magn Reson Imaging*. 2016;**34**(4):596–602. [PubMed ID: 26708035]. [PubMed Central ID: PMC4801649]. https://doi.org/10.1016/j.mri.2015.12.006.
19. Zhang YZ, Chang C, Wei XE, Fu JL, Li WB. Comparison of diffusion tensor image study in association fiber tracts among normal, amnestic mild cognitive impairment, and Alzheimer's patients. *Neurol India*. 2011;**59**(2):168–73. [PubMed ID: 21483111]. https://doi.org/10.4103/0028-3886.79129.
20. Thomas AA, Fisher JL, Hampton TH, Christensen BC, Tsongalis GJ, Rahme GJ, et al. Immune modulation associated with vascular endothelial growth factor (VEGF) blockade in patients with glioblastoma. *Cancer Immunol Immunother*. 2017;**66**(3):379–89. [PubMed ID: 27942839]. https://doi.org/10.1007/s00262-016-1941-3.
21. Osterberg N, Ferrara N, Vacher J, Gaedicke S, Niedermann G, Weyerbrock A, et al. Decrease of VEGF-A in myeloid cells attenuates glioma progression and prolongs survival in an experimental glioma model. *Neuro Oncol*. 2016;**18**(7):939–49. [PubMed ID: 26951383]. [PubMed Central ID: PMC4896547]. https://doi.org/10.1093/neuonc/now005.
22. Zhou Y, Jin G, Mi R, Zhang J, Zhang J, Xu H, et al. Inhibition of fatty acid synthase suppresses neovascularization via regulating the expression of VEGF-A in glioma. *J Cancer Res Clin Oncol*. 2016;**142**(12):2447–59. [PubMed ID: 27601165]. https://doi.org/10.1007/s00432-016-2249-6.
23. Su C, Liu C, Zhao L, Jiang J, Zhang J, Li S, et al. Amide Proton Transfer Imaging Allows Detection of Glioma Grades and Tumor Proliferation: Comparison with Ki-67 Expression and Proton MR Spectroscopy Imaging. *AJNR Am J Neuroradiol*. 2017;**38**(9):1702–9. [PubMed ID: 28729292]. [PubMed Central ID: PMC7963688]. https://doi.org/10.3174/ajnr.A5301.
24. Martino J, Mato D, de Lucas EM, García-Porrero JA, Gabarrós A, Fernández-Coello A, et al. Subcortical anatomy as an anatomical and functional landmark in insulo-opercular gliomas: implications for surgical approach to the insular region. *J Neurosurg*. 2015;**123**(4):1081–92. [PubMed ID: 25955870]. https://doi.org/10.3171/2014.11.jns141992.
25. Engelhorn T, Schwarz MA, Hess A, Budinsky L, Pitann P, Eyüpoglu I, et al. Definition of K(trans) and FA thresholds for better assessment of experimental glioma using high-field MRI: a feasibility study. *Clin Neuroradiol*. 2014;**24**(4):337–45. [PubMed ID: 24346229]. https://doi.org/10.1007/s00062-013-0257-3.
26. Aliotta E, Nourzadeh H, Batchala PP, Schiff D, Lopes MB, Druzgal JT, et al. Molecular Subtype Classification in Lower-Grade Glioma with Accelerated DTI. *AJNR Am J Neuroradiol*. 2019;**40**(9):1458–63. [PubMed ID: 31413006]. [PubMed Central ID: PMC7048441]. https://doi.org/10.3174/ajnr.A6162.
27. Jiang L, Yao Z, Feng X, Wang Y, Jiang S, Yang Z. Evaluation of DTI parameters for glioma grading and correlation with tumor proliferation. *Chin Comput Med Imaging*. 2013;**19**(2):106–10.